



Chemical depletion of phagocytic immune cells in *Anopheles gambiae* reveals dual roles of mosquito hemocytes in anti-*Plasmodium* immunity

Hyeogsun Kwon^a and Ryan C. Smith^{a,1}

^aDepartment of Entomology, Iowa State University, Ames, IA 50011

Edited by Carolina Barillas-Mury, National Institutes of Health, Bethesda, MD, and approved June 5, 2019 (received for review January 7, 2019)

Mosquito immunity is composed of both cellular and humoral factors that provide protection from invading pathogens. Immune cells known as hemocytes, have been intricately associated with phagocytosis and innate immune signaling. However, the lack of genetic tools has limited hemocyte study despite their importance in mosquito anti-*Plasmodium* immunity. To address these limitations, we employ the use of a chemical-based treatment to deplete phagocytic immune cells in *Anopheles gambiae*, demonstrating the role of phagocytes in complement recognition and prophenoloxidase production that limit the ookinete and oocyst stages of malaria parasite development, respectively. Through these experiments, we also define specific subtypes of phagocytic immune cells in *An. gambiae*, providing insights beyond the morphological characteristics that traditionally define mosquito hemocyte populations. Together, this study represents a significant advancement in our understanding of the roles of mosquito phagocytes in mosquito vector competence and demonstrates the utility of clodronate liposomes as an important tool in the study of invertebrate immunity.

Anopheles gambiae | innate immunity | hemocytes | malaria | phagocyte depletion

Innate immune defenses are essential for combating infectious pathogens throughout the animal kingdom (1). In insects, innate immunity is composed of cellular and humoral components that coordinate killing responses through phagocytosis, melanization, and pathogen lysis. Immune cells, known as hemocytes, are integral to both cellular and humoral responses, respectively serving in direct or indirect roles to limit pathogen survival. Much of our understanding of insect hemocyte biology has relied on the genetics of *Drosophila melanogaster* to delineate hematopoiesis, immune cell function, and their contributions to innate immunity (2–4), serving as an integral model for less characterized invertebrate systems. In mosquitoes, 3 circulating hemocyte subtypes have been characterized largely by morphology with limited biochemical or genetic characterization (5–7). Functionally analogous to vertebrate macrophages, mosquito granulocytes are characterized by their phagocytic ability and adherence to tissues or foreign surfaces (6, 7). Oenocytoids have primarily been implicated in the production of phenoloxidases (POs) that lead to melanization responses (6–8), while prohemocytes are hypothesized to function as progenitor cells or as potentially smaller cells with phagocytic ability (6, 9).

Previous studies have demonstrated that *Anopheles gambiae* hemocytes respond to blood feeding (10–12), as well as bacterial and malaria parasite challenge (6, 13), eliciting changes in their cellular profiles at the transcriptional (14, 15) and proteome levels (16). This has led to the identification of several mosquito hemocyte components with integral roles in phagocytosis (17, 18) and anti-*Plasmodium* immunity (14, 16, 19). In addition, hemocyte differentiation in response to malaria parasite challenge has been described as an integral requirement of mosquito immune priming (20–22) and immune responses targeting *Plasmodium* oocyst survival (23–25). However, studies of mosquito immune cell function have been severely limited by the lack of genetic

tools to better understand the contributions of individual hemocyte subtypes to mosquito innate immune function.

To overcome these limitations, we employed clodronate liposomes (CLDs) to chemically deplete phagocytic cell populations in *Anopheles gambiae* using widely established techniques from mammalian systems to ablate macrophage populations (26–28). By applying this methodology, we take advantage of the phagocytic properties of mosquito immune cells to better understand their functional contributions to pathogen challenge and anti-*Plasmodium* immunity. Following CLD treatment, phagocyte depletion was confirmed using multiple methods of validation (light microscopy, flow cytometry, qRT-PCR, and immunofluorescence assays) and negatively impacted mosquito survival following bacterial challenge. In addition, phagocyte depletion notably impaired *Plasmodium* killing responses at both the ookinete and oocyst stages, providing mechanistic understanding into the immune components that influence parasite survival in the mosquito host. Together, these data represent a significant advancement in the study of invertebrate immune cell function, as well as define integral roles of phagocytic immune cells in mosquito anti-*Plasmodium* immunity.

Results

Phagocyte Depletion Using Clodronate Liposomes. To understand the roles of phagocytic immune cells in mosquito immunity, CLDs were employed to chemically deplete phagocytes in *An. gambiae*

Significance

The mosquito immune system is an integral determinant of vector competence. Immune cells, known as hemocytes, have been implicated in limiting malaria parasite survival, yet the lack of genetic tools has limited their study. Herein, we employ clodronate liposomes to selectively deplete mosquito phagocytic immune cells to better define their contributions to parasite killing. We demonstrate that phagocytic cells contribute to mosquito complement recognition of invading ookinetes and limit oocyst survival through the production of prophenoloxidases, providing insights into the mechanisms of malaria parasite killing. In addition, these experiments have enabled the identification of multiple phagocytic cell types in *Anopheles gambiae*, demonstrating the potential of this methodology as a valuable tool for the study of invertebrate immunology.

Author contributions: H.K. and R.C.S. designed research; H.K. performed research; H.K. and R.C.S. analyzed data; and H.K. and R.C.S. wrote the paper.

The authors declare no conflict of interest.

This article is a PNAS Direct Submission.

Published under the PNAS license.

Data deposition: The data reported in this paper have been deposited in the Gene Expression Omnibus (GEO) database, <https://www.ncbi.nlm.nih.gov/geo> (accession no. GSE116156).

¹To whom correspondence may be addressed. Email: smithr@iastate.edu.

This article contains supporting information online at www.pnas.org/lookup/suppl/doi:10.1073/pnas.1900147116/-DCSupplemental.

Published online June 24, 2019.

(SI Appendix, Fig. S1A). Widely used in studies of mammalian immunity (26–28), CLDs were injected into adult female mosquitoes to titer the required concentration of liposomes needed for depletion. From these experiments, a 1:5 dilution of CLDs in 1× PBS was chosen for its efficacy in ablating phagocytes without negative impacts on mosquito survival (SI Appendix, Fig. S1B). To determine the efficacy of cell depletion, granulocyte populations were evaluated from naive, blood-fed, or *Plasmodium berghei*-infected mosquitoes based on morphology (SI Appendix, Fig. S2A) using a hemocytometer as previously (22, 23). Clodronate treatment reduced the percentage of granulocytes by ~40% in naive mosquitoes when examined at either 24 or 48 h (SI Appendix, Fig. S3) yet did not reduce other hemocyte subtypes (SI Appendix, Fig. S4). Higher levels of depletion (~90%) were observed in blood-fed or *P. berghei*-infected samples (SI Appendix, Fig. S3). This increase in phagocyte depletion may be attributed to the enhanced phagocytic ability and capacity following the physiological changes that accompany blood feeding (SI Appendix, Fig. S5), presumably enabling a higher dosage of clodronate to the cell. Depletion was further validated by immunofluorescence of fixed hemocyte populations stained with DiI and wheat germ agglutinin (WGA), which have both previously served as “universal markers” to label hemocyte populations (SI Appendix, Fig. S2B; refs. 2, 10, 20, and 26), demonstrating that immune cell populations were significantly reduced in CLD-treated mosquitoes compared with liposome controls (Fig. 1A). These morphological data support that granulocyte populations are significantly reduced following clodronate treatment.

Additional validation of phagocyte depletion was performed by examining the transcripts of two well-characterized genes associated with hemocyte phagocytic function, *eater* and *nimrod B2* (29–32) by qRT-PCR. The relative transcript abundance of *eater* and *nimrod B2* was significantly reduced in CLD-treated mosquitoes compared with control liposome under each experimental condition (Fig. 1B). Based on previous work isolating phagocytic immune cells by their phagocytic properties (16), we also utilized a similar approach to further distinguish the effects of clodronate treatment on phagocytic cells by flow cytometry analyses (SI Appendix, Fig. S2C). Using fluorescent beads to distinguish phagocytic cells (SI Appendix, Fig. S5; ref. 33), phagocytic cell populations could effectively be measured and compared between treatments using strict size cutoffs and signal thresholds (SI Appendix, Fig. S6). Flow cytometry analyses revealed that CLD treatment significantly depleted mosquito phagocyte populations under naive, blood-fed, and *P. berghei*-infected conditions (Fig. 1C and SI Appendix, Fig. S7). Similar to our light microscopy results (SI Appendix, Fig. S3), the efficacy of phagocyte depletion is increased following a blood meal, independent of infection status (Fig. 1C). Together, these data provide strong support for the chemical depletion of mosquito phagocytic immune cells using CLDs.

In addition, our flow cytometry data argue that there are at least two distinct populations of phagocytic immune cells in *An. gambiae*. Under each experimental condition, phagocytic cells were noticeably segregated into upper and lower phagocyte populations (Fig. 1C and SI Appendix, Fig. S8A). Across feeding status, an upper population was more susceptible to CLD treatment, displaying significant reduction in the percentage of phagocytic cells. This is in contrast to the lower phagocyte population, which displayed little response to CLD treatment (SI Appendix, Fig. S8A). Further quantification of these upper and lower populations by size (forward scatter [FSC]) and granularity (side scatter [SSC]) demonstrate size differences under naive conditions and significant disparities in granularity across feeding status (SI Appendix, Fig. S8B). Similar comparisons between control and CLD treatments display no major differences between these upper and lower populations (SI Appendix, Fig. S8C). These data suggest that the upper and lower populations

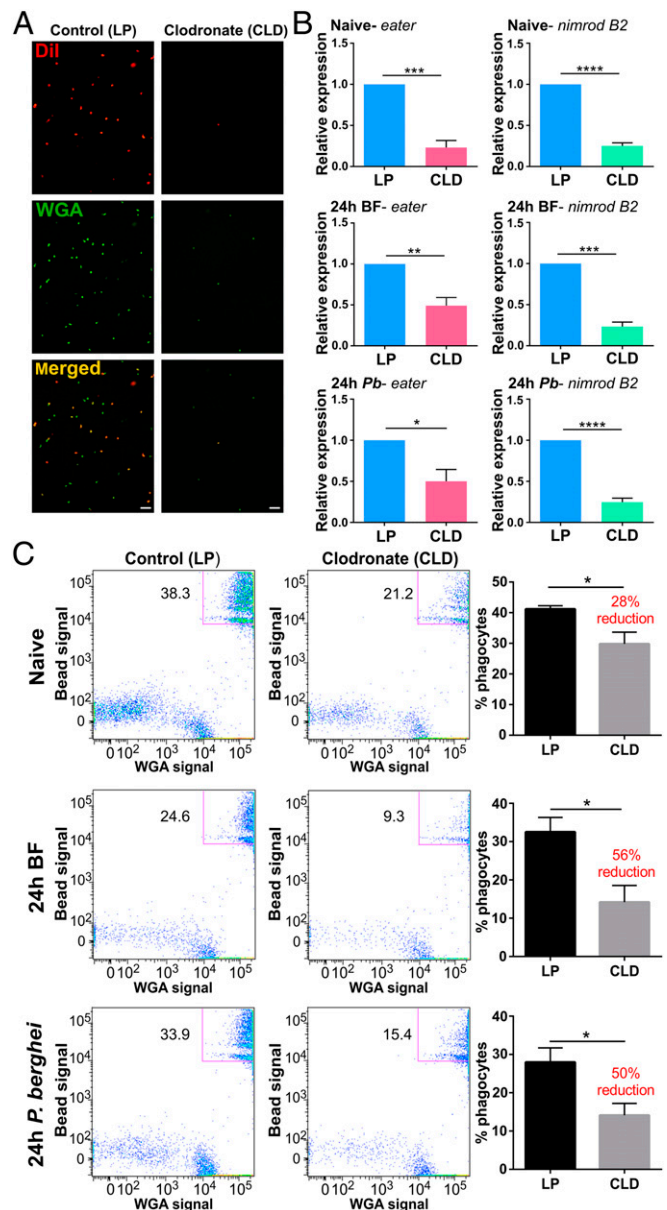


Fig. 1. Mosquito phagocytes are significantly depleted following clodronate liposome (CLD) treatment. Following the injection of control (LP) or clodronate liposomes (CLD), mosquitoes were challenged with *P. berghei* and hemocytes were perfused 24 h postinfection. Hemocytes were stained with the hemocyte-specific markers, DiI (red) and WGA (green), to visualize the effects of CLD treatment on hemocyte populations (A). Additional experiments with molecular markers of phagocytic cells, *eater* and *nimrod B2*, were used to further evaluate phagocyte depletion. Relative transcript levels of *eater* and *nimrod B2* expression were significantly reduced in CLD-treated mosquitoes (B). Further validation was performed using flow cytometry to confirm the depletion of phagocytic hemocyte populations under naive, 24-h blood-fed (24-h BF), and 24-h *P. berghei*-infected (24-h *P. b.*) conditions (C). Representative flow cytometry experiments display the depletion of phagocytic hemocytes (as determined by the uptake of fluorescent beads and WGA staining), with bar graphs depicting a significant decrease in phagocytes following CLD treatment from 3 independent experiments (C). Blood-feeding, independent of pathogen challenge, caused phagocytes to be more susceptible to CLD treatment (C). Bars represent mean \pm SEM of 3 independent replicates. Data were analyzed by unpaired *t* test using GraphPad Prism 6.0. Asterisks denote significance (**P* < 0.05, ***P* < 0.01, ****P* < 0.001, *****P* < 0.0001). (Scale bar: 20 μ m.)

comprise distinct cell types with different phagocytic capacity, which may explain why the upper cell population with increased phagocytic activity results in a stronger depletion following CLD treatment.

Phagocyte Depletion Increases Susceptibility to Bacterial Infections.

To determine the influence of phagocyte depletion on immune function and host survival, control and CLD liposome-treated mosquitoes were challenged with bacteria. Injury alone had no effect on mosquito survival (Fig. 2A), while challenging with either gram (+) or gram (–) bacteria had notable impacts on survival (Fig. 2). However, phagocyte depletion significantly decreased mosquito survival to *Serratia marcescens* (Fig. 2B) and *Staphylococcus aureus* challenge (Fig. 2C). Given the importance of phagocytic cells as immune sentinels required to remove invading pathogens (30, 32, 34), these experiments further demonstrate the effects of clodronate depletion and the important contributions of phagocytes as critical effectors of mosquito cellular immunity.

Phagocyte Depletion Impairs “Early-Phase” and “Late-Phase” Mosquito Immunity.

Several studies have implicated hemocytes in anti-*Plasmodium* immunity (14, 16, 18, 20, 22, 23, 35), yet the specific contributions of phagocytic immune cells in these immune responses have remained elusive. To define the specific contributions of phagocytes on malaria parasite survival, control and CLD-treated mosquitoes were challenged with *P. berghei* infection (Fig. 3). Phagocyte depletion significantly increased mature oocyst numbers at day 10 (Fig. 3A), indicating that phagocytes serve as critical determinants of parasite survival. When further examined temporally, early oocyst numbers were significantly increased 2 d postinfection (Fig. 3B). With integral roles in ookinete lysis (36–38), we examined TEP1 expression in mosquito hemolymph in control and clodronate-treated mosquitoes (Fig. 3C). TEP1 protein levels in naive or *P. berghei*-infected mosquito hemolymph were not influenced by phagocyte depletion (Fig. 3C); however, in CLD-treated mosquitoes, TEP1 binding to invading ookinetes was significantly impaired (Fig. 3D). These data argue that mosquito phagocytes mediate TEP1 recognition of invading ookinetes, and are supported by recent findings arguing that hemocyte-derived microvesicles deliver critical factors needed to establish mosquito complement binding to the ookinete surface (35).

Previous work has also demonstrated the integral role of hemocytes in defining oocyst survival (23, 24). To examine the effects of phagocyte depletion on oocyst numbers, early and late oocyst numbers were measured. In control mosquitoes, oocysts were significantly reduced between day 2 and day 8 (Fig. 3E)

similar to previous descriptions of mosquito late-phase immunity (23–25, 39). However, in CLD-treated mosquitoes, oocyst numbers remained constant between day 2 and day 8 (Fig. 3F), suggesting that phagocytes contribute to both early- and late-phase immune responses that limit parasite numbers in the mosquito host.

Further experiments in which mosquitoes were treated with CLD ~24 h after *P. berghei* challenge demonstrate that there are temporal aspects to anti-*Plasmodium* immunity. In contrast to the results of Fig. 3A, phagocyte depletion after ookinete invasion had no effect on oocyst survival (Fig. 3G), although phagocytes were significantly depleted following an established infection (SI Appendix, Fig. S9). This suggests that phagocyte-mediated immune responses are induced shortly after ookinete invasion (<24 h), which once initiated, mosquito phagocytes are no longer required.

RNA-Seq Reveals Changes in Gene Expression Associated with Phagocyte Depletion.

Evidence from *Drosophila* argues that hemocyte-derived signals are required to initiate humoral immune responses (40, 41), which may similarly contribute to anti-*Plasmodium* immunity in the mosquito host. Following this methodology, RNA-seq analysis was performed on control and CLD-treated mosquito carcass samples 24 h after *P. berghei* infection. To our surprise, only 50 transcripts were differentially regulated (SI Appendix, Table S1) (42), of which the majority had annotated immune function (Fig. 4A). This included the known phagocyte proteins LRIM 16A, LRIM 16B, and nimrod B2 (16), as well as several other leucine rich-repeat (*LRR*) proteins, fibrinogens, and multiple prophenoloxidase (*PPO*) genes that were significantly down-regulated following CLD treatment (Fig. 4B). Validation of the RNA-seq data by qRT-PCR produced comparable levels of gene expression and a significant correlation ($R^2 = 0.94$) between both types of analyses (SI Appendix, Fig. S10).

PPO Expression and PO Activity Are Significantly Reduced following Phagocyte Depletion.

With the identification of multiple PPO transcripts influenced by phagocyte depletion (Fig. 4B), we further explored the expression of all annotated PPO genes. All 9 PPO genes displayed a significant reduction in their expression in carcass samples (Fig. 4C), similar to our RNA-seq analysis. In contrast, when perfused hemocytes were examined (Fig. 4D), only PPO-2, -3, -8, and -9 expression was significantly reduced following CLD treatment. This argues that some PPOs may still be expressed in circulating hemocytes. As precursors of melanization reactions in insects (43), PO activity was measured in perfused hemolymph samples from control and CLD-treated

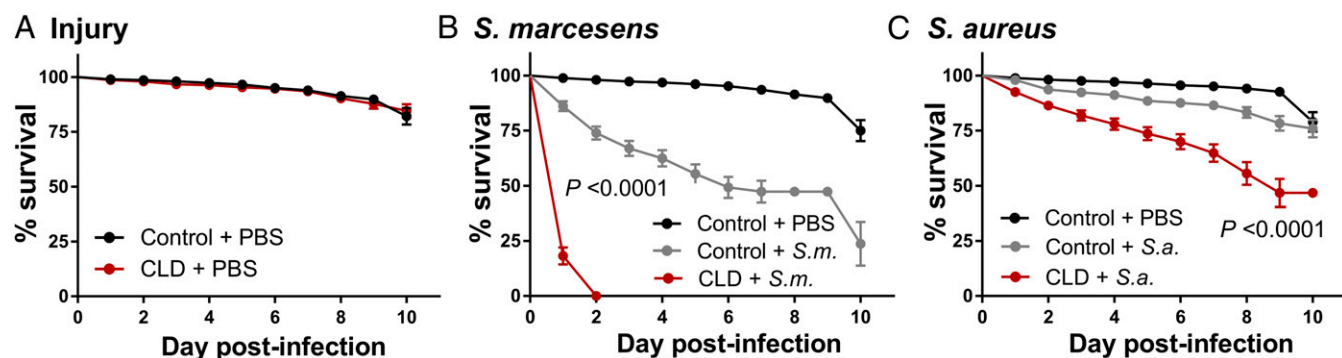


Fig. 2. Depletion of phagocytic cells influences mosquito survival after bacterial challenge. Mosquitoes were treated with either control or CLDs, and then subjected to injury (sterile PBS injection) or bacterial challenge. Survivorship was monitored in mosquitoes every day for 10 d to evaluate the effects of injury (A), *S. marcescens* (B), or *S. aureus* (C) challenge. Phagocyte depletion (CLD) in mosquitoes results in a high susceptibility to bacterial infections. Error bars represent the mean \pm SEM of 3 independent replicates. In each replicate, 30 female mosquitoes were used for each experimental treatment. Data were analyzed by a log-rank (Mantel-Cox) test using GraphPad Prism 6.0.

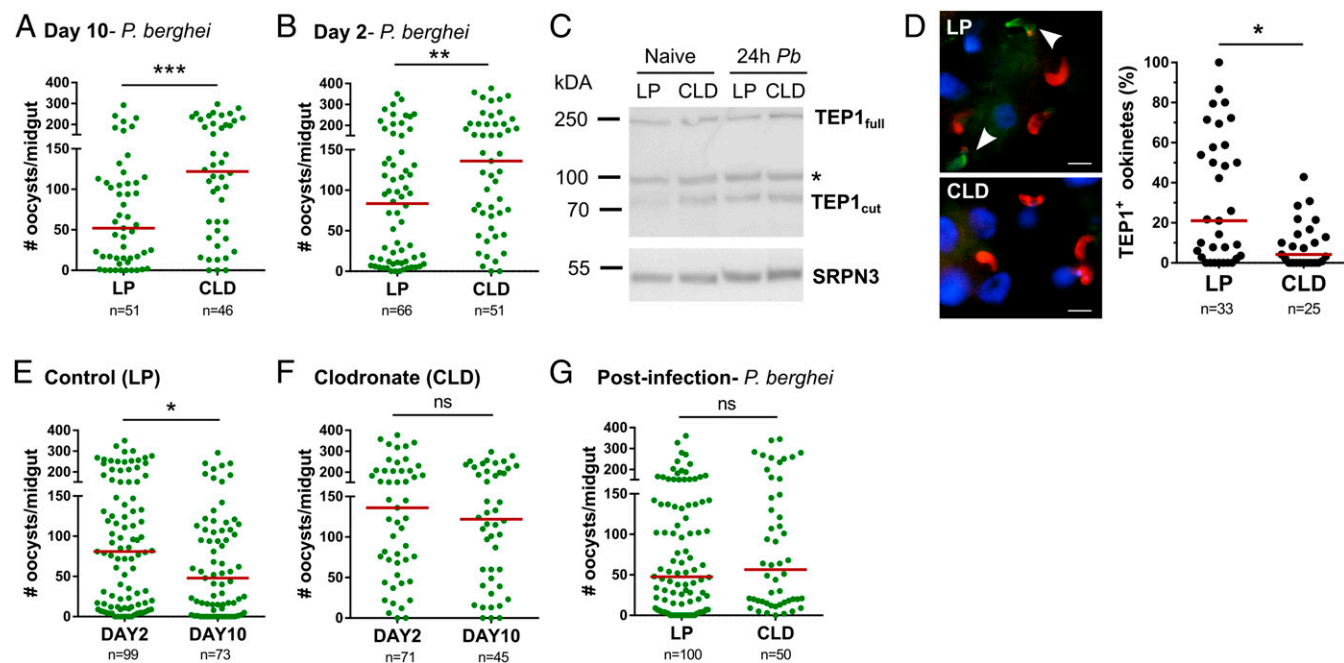


Fig. 3. Effects of phagocyte depletion on *P. berghei* development. One day before challenge with *P. berghei* (pretreatment), mosquitoes were treated with control (LP) or clodronate liposomes (CLD). Ten days postinfection, *Plasmodium* oocyst numbers were evaluated to determine the effects of phagocyte depletion on malaria parasite numbers (A). To determine the temporal components that influence this increase in parasite survival, day 2 early oocyst numbers were examined in LP- and CLD-treated mosquitoes (B). Although phagocyte depletion increased early oocyst numbers, levels of TEP1 protein did not differ between LP and CLD treatments in either naive or 24-h *P. berghei*-infected hemolymph samples where serpin 3 (SRPN3) was used as a protein loading control (C). Nonspecific bands were denoted by an asterisk. Evaluation of TEP1 binding to invading ookinetes (~22–24 h post-*P. berghei* infection) by immunofluorescence after phagocyte depletion demonstrates that TEP1 binding (green; indicated by arrows) to ookinetes (α -Pbs 21; red) is significantly impaired (D). To examine oocyst survival, oocyst numbers were examined at 2 and 10 d post-*P. berghei* infection in mosquitoes treated with control liposomes (E) or CLDs (F). Oocyst numbers were measured by fluorescence using the same cohort of mosquitoes for both time points. Clodronate treatment after the establishment of infection (24 h post-*P. berghei* infection) had no effect on malaria parasite survival (G). Three or more independent experiments were performed for all infection experiments, and data were analyzed using Mann–Whitney test with GraphPad Prism 6.0. Median oocyst numbers are indicated by the horizontal red line, and asterisks denote significance (* $P < 0.05$, ** $P < 0.01$, *** $P < 0.001$); ns, not significant; n , number of midguts examined.

mosquitoes. Forty-eight hours posttreatment, PO activity was significantly reduced in naive CLD-treated mosquitoes after 60 min (Fig. 4E). The influence of blood feeding amplified these responses, reducing PO activity across all sample time points (Fig. 4E). Similarly, PO activity was reduced following *P. berghei* infection and produced lower levels by comparison with a non-infected blood meal (Fig. 4E). These data imply that PPO expression and subsequent PO activity are impaired following phagocyte depletion.

Multiple PPOs Influence *Plasmodium* Oocyst Survival. Based on the RNA-seq results and reduced PO activity in CLD-treated mosquitoes (Fig. 4), we examined several candidate immune genes that featured prominently in our analyses to determine their respective contributions to *Plasmodium* survival. This included *CLIPD1*, a putative leucine-rich immune (LRIM) protein (AGAP001470), as well as multiple PPO genes (*PPO-2*, *-3*, *-4*, *-5*, *-6*, and *-9*). All 8 candidate genes were significantly silenced following the injection of dsRNA (SI Appendix, Fig. S11). As members of a multigene family, the specificity of PPO silencing was further verified using specific primers for each of the 9 PPO genes in *An. gambiae* (SI Appendix, Fig. S12). RNA interference (RNAi) specifically targeted *PPO2*, *PPO4*, *PPO5*, and *PPO6*, while *PPO3* and *PPO9* had unintended off-target effects on 1 or more PPO genes (SI Appendix, Fig. S12). The loss of *CLIPD1*, *AGAP001470*, *PPO4*, *PPO5*, and *PPO6* had no effect on parasite numbers (SI Appendix, Fig. S13), while silencing *PPO2*, *PPO3*, or *PPO9* increased the intensity of malaria parasite infection (Fig. 5A). However, when early oocyst numbers were examined at day 2, *PPO2*, *PPO3*, and *PPO9* silencing

did not influence ookinete invasion success (Fig. 5B). This argues that *PPO2*, *PPO3*, and *PPO9* contribute to oocyst survival similar to previous reports (23, 24, 39), suggesting that PPOs are important determinants of oocyst survival.

Analyses of PPO6 Protein Expression in Phagocytes. Although *PPO6* silencing does not produce a discernable oocyst phenotype, several reports have described PPO6 as a reliable marker of mosquito hemocytes (11, 12, 44, 45) and phagocytes (16, 45). Following CLD treatment, the number of circulating PPO6⁺ phagocytes are significantly depleted (Fig. 6A), resulting in a higher proportion of nonphagocytic PPO6⁺ cells comprising the remaining immune cell population (Fig. 6B). This provides support that a subset of PPO6⁺ phagocytes are depleted by CLD treatment (Fig. 6C), while other phagocytic and nonphagocytic PPO6⁺ cell types are unaffected (Fig. 6). The levels of PPO6 in mosquito hemolymph remain unchanged after CLD treatment (SI Appendix, Fig. S14), suggesting that these unaffected immune cell subtypes, likely oenocytoids that have primarily been implicated in PPO production, may be responsible for the majority of PPO6 in the hemolymph. This is supported by the unchanged *PPO6* transcript levels in circulating hemocytes following clodronate treatment (Fig. 4D).

Similar to Severo et al. (45), we identify immune cell populations that significantly vary in their expression of PPO6 (SI Appendix, Fig. S15). These populations were characterized by their PPO6 expression levels (defined as either PPO6^{high} or PPO6^{low}; SI Appendix, Fig. S15), phagocytic or nonphagocytic properties, and morphological features (elongated/spread or

rounded) to further define these cell populations following phagocyte depletion (Fig. 6C). CLD treatment was most effective in reducing populations of PPO6^{low} cells with elongated or spread morphologies (Fig. 6C), phenotypes most commonly associated with mosquito granulocytes. PPO6^{high} phagocytic cell populations were also significantly reduced following CLD treatment, yet these cell types comprise a much smaller proportion of the phagocytic cell population (Fig. 6C). Interestingly, small, rounded PPO6^{low} phagocytic cells similar to those described by King and Hillyer (9), comprised the majority of phagocytic cells following CLD treatment (Fig. 6C). Based on these results, this small PPO6^{low} phagocytic cell population may

be less susceptible to CLD treatment and likely comprise the “lower” cell population described in our flow cytometry analysis (*SI Appendix*, Fig. S8). Together, these data argue that CLDs can specifically deplete distinct subpopulations of phagocytic immune cells in the mosquito host and provide insight into the complexity of mosquito phagocyte populations.

Discussion

Over the last decade, we have gained significant insights into the biology of mosquito hemocytes and their respective roles in innate immune function. From gene and protein expression studies (14–16), an extensive catalog of the molecular responses to blood

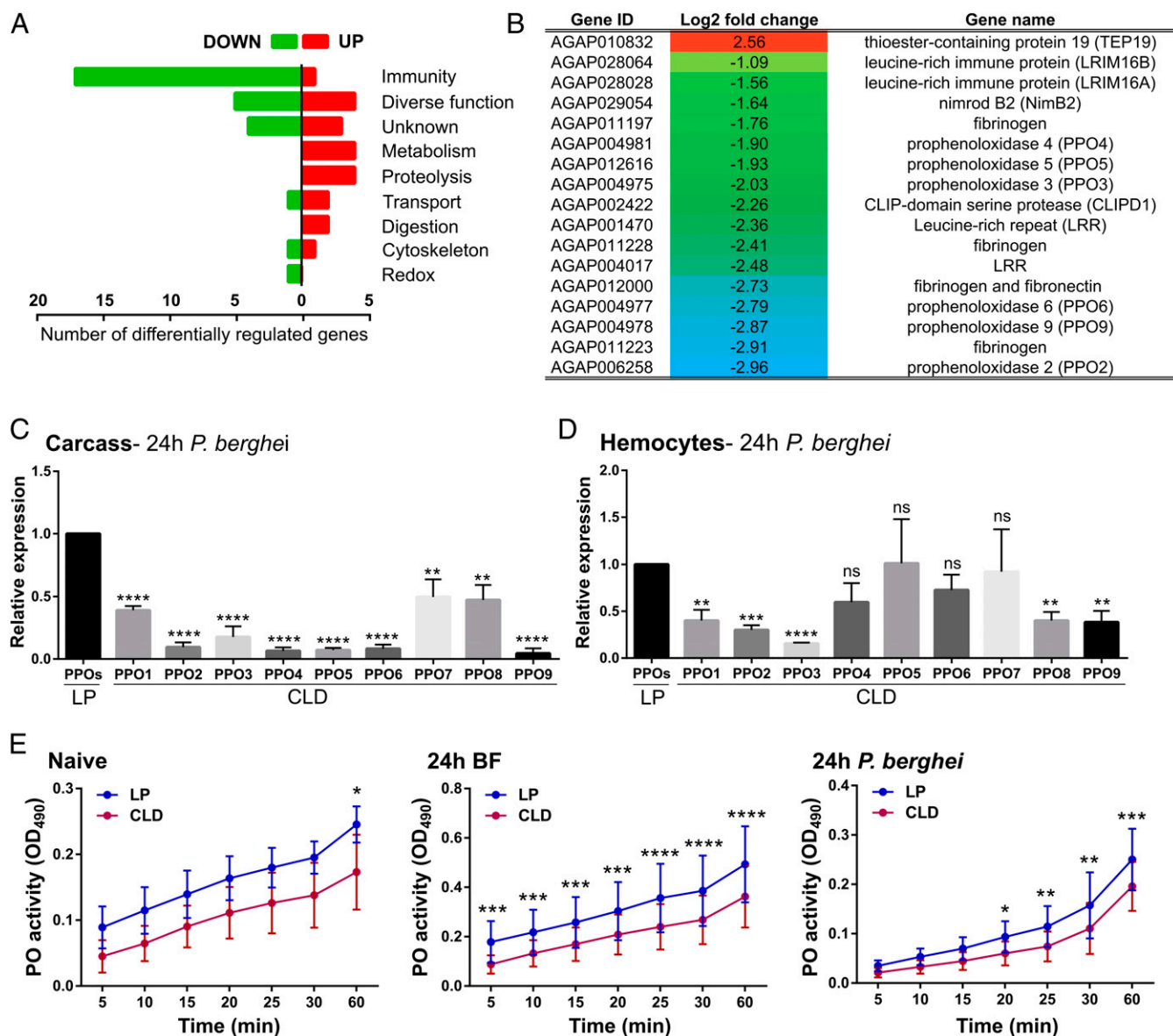


Fig. 4. Phagocyte depletion reduces prophenoloxidase (PPO) expression. RNA-seq analyses following clodronate treatment revealed 50 differentially regulated genes in abdomen tissues 24 h post-*P. berghei* infection and grouped by gene ontology (A). Comprising the largest category of affected genes, the annotations and log₂fold change of specific immune genes with significant differential regulation are displayed (B). This includes several PPO genes, therefore leading us to examine the expression of all 9 PPO family members by qRT-PCR analyses in the carcass (C) and hemocyte (D) samples in control liposome (LP) and clodronate-treated (CLD) samples. Data were analyzed using an unpaired *t* test to determine differences in relative gene expression of each respective PPO gene between LP and CLD treatments (C and D). Due to the importance of PPOs in phenoloxidase (PO) activation, PO activity was measured in hemolymph samples derived from LP and CLD samples in naive, blood-fed, and *P. berghei*-infected conditions (E). Measurements (OD₄₉₀) were taken for DOPA conversion assays at 5-min intervals from 0 to 30 min, and then again using a final readout at 60 min. Data were analyzed using a two-way repeated-measures ANOVA followed by Sidak's multiple comparisons using GraphPad Prism 6.0. Bars represent mean \pm SEM of 3 independent experiments. Asterisks denote significance (**P* < 0.05, ***P* < 0.01, ****P* < 0.001, *****P* < 0.0001).

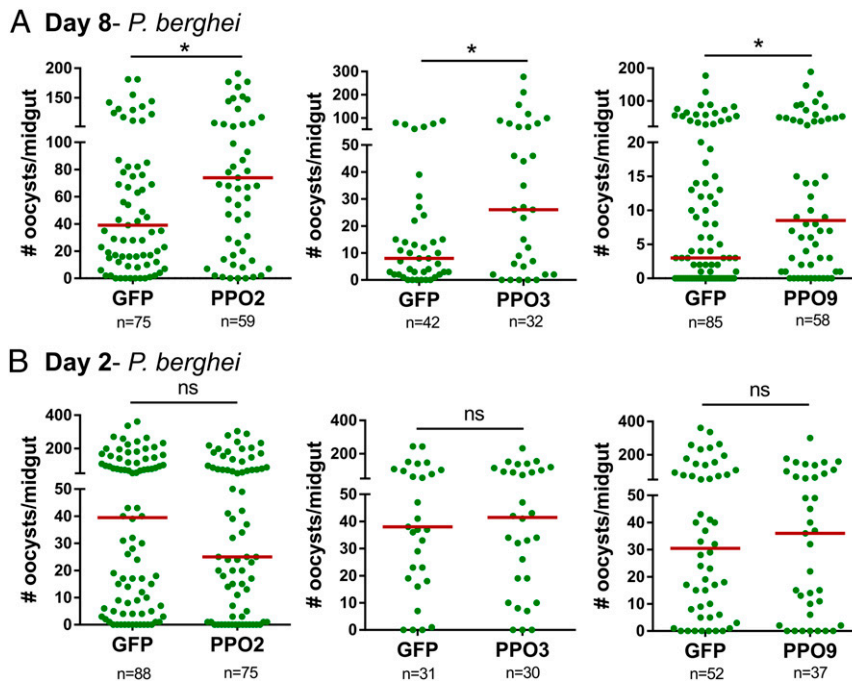


Fig. 5. The silencing of PPOs influences *Plasmodium* oocyst survival. The influence of *PPO2*, *PPO3*, and *PPO9* silencing on *Plasmodium* oocysts numbers in *An. gambiae* was evaluated 8 d postinfection compared with dsGFP controls (A). To determine whether gene silencing influences the success of ookinete invasion, similar experiments were performed in which early oocyst numbers were used as a readout of ookinete survival 2 d postinfection (B). For all experiments, each dot represents the number of parasites on an individual midgut, with the median value denoted by a horizontal red line. Data were pooled from 3 or more independent experiments with statistical analysis determined by a Mann–Whitney test using GraphPad Prism 6.0. Asterisks denote significance (* $P < 0.05$, *** $P < 0.001$).

feeding and pathogen challenge has been produced. New information into the impacts of physiology on mosquito immune cell dynamics (10–12), infection-induced interactions of circulating hemocytes (9, 13, 46), and the role of hemocytes as important modulators of anti-*Plasmodium* immunity (14, 16, 19, 20, 22, 23, 35) has been addressed. However, the functional classifications of these mosquito immune cell populations have been severely limited by the lack of genetic tools and molecular markers.

In *Drosophila*, 3 immune cell types have been described (plasmatocyte, crystal cells, and lamellocytes) that emerge from the progenitor cells of two distinct myeloid lineages (2, 47, 48). The genetic resources available in *Drosophila* have enabled a well-developed system for the study of hemocyte populations through a variety of mutant and transgenic lines (49–53). Similar to our own study, a *domino* mutant has been described in which hemocytes are absent (49, 50). Additional studies have also expressed proapoptotic proteins in hemocytes, causing the ablation of all circulating immune cells or specific cell subtypes (51, 52). Together, these studies have been instrumental to understanding the roles of *Drosophila* hemocytes to injury and innate immune signaling (50–52). However, the lack of genetic tools has made similar hemocyte studies in mosquitoes and other insects difficult.

Mosquito hemocytes have been broadly characterized as prohemocytes, oenocytoids, and granulocytes relying primarily on morphological identification and homology to other invertebrate systems (6, 7). Of these cell types, granulocytes have been the most well-studied for their distinct shape and phagocytic properties, resulting in the identification of several immune molecules with integral roles in phagocytosis (17, 18). These phagocytic properties have enabled the proteomic study of mosquito phagocytes (16) and have served as our motivation to selectively target phagocytic cell populations using CLDs in *An. gambiae*.

In mammalian systems, CLDs have been widely used to deplete vertebrate macrophage populations (26–28). Upon phagocytosis, liposome particles are degraded by the endosome,

releasing clodronate that promotes apoptosis and the loss of phagocytic cells (26, 27). Herein described in an invertebrate system, we demonstrate that CLDs can effectively deplete phagocytic cell populations in the malaria vector, *An. gambiae*, and validate their depletion through a variety of cellular- and molecular-based approaches. Light microscopy and immunofluorescence assays argue that granulocyte populations are significantly reduced following CLD treatment. This is further supported by the decrease in *eater* and *nimrod B2* transcripts that are routinely associated with phagocytic hemocytes in mosquitoes (31, 32) and other Diptera (29, 30). Additional validation by flow cytometry confirm the effects of clodronate treatment on phagocyte depletion, revealing at least two phagocytic cell populations in mosquitoes with varied susceptibility to clodronate treatment. When combined with levels of PPO6 staining following CLD treatment, our data suggest that 3 or more phagocyte populations are present in *An. gambiae*. This includes highly phagocytic PPO6⁺ and PPO6⁻ cell types, similar to those previously described (45), that are susceptible to phagocyte depletion. An additional small, rounded PPO6⁻ phagocytic cell similar to those described by King and Hillyer (9), displayed little response to CLD treatment. Together, these data provide strong evidence that CLDs can deplete mosquito phagocytic granulocyte cell populations, providing insights into previously undescribed complexities of mosquito phagocyte populations. However, due to previous observations that oenocytoids can internalize beads and bacteria (54), we cannot conclusively rule out the potential that oenocytoids may also be influenced by clodronate treatment.

From these experiments, we also provide evidence that the efficacy of clodronate treatment is influenced by mosquito physiology. Phagocyte depletion was much more effective following blood feeding, independent of pathogen challenge. This is in agreement with the increased cellular activity and up-regulation of immune-related molecules in hemocytes following

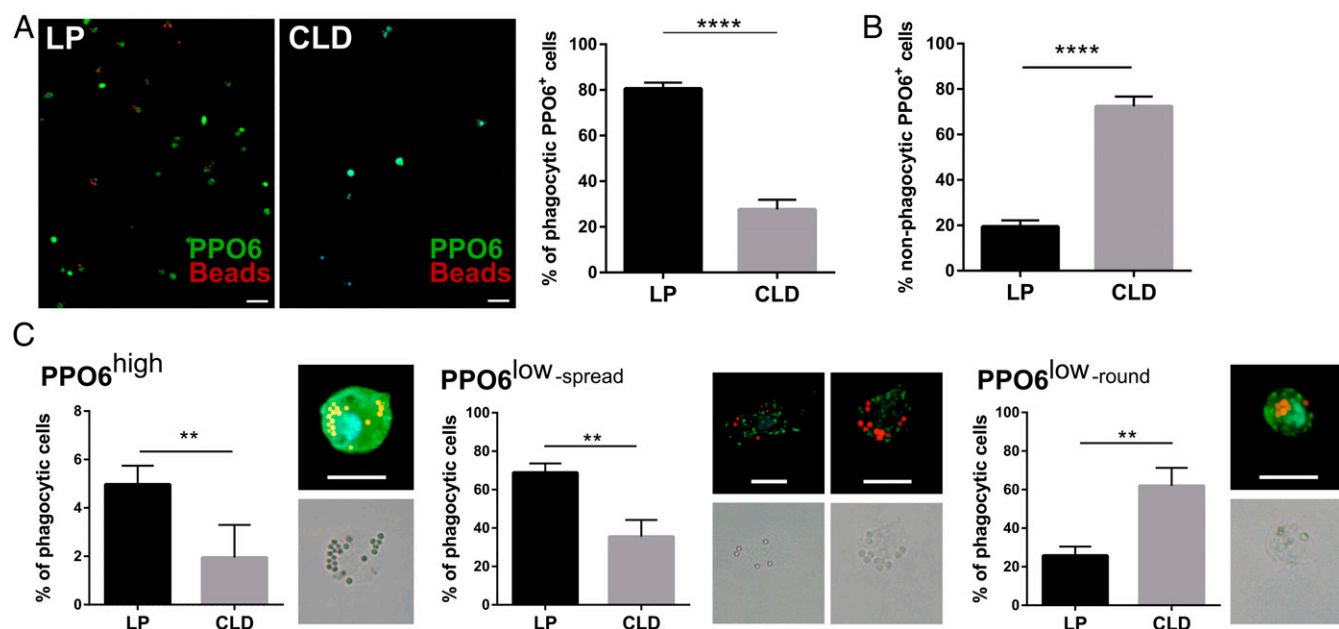


Fig. 6. Clodronate treatment differentially impacts mosquito phagocyte subpopulations. PPO6 staining was evaluated by immunofluorescence in perfused hemocytes after the injection of fluorescent beads from control liposome (LP) or clodronate-treated (CLD) mosquitoes ~24 h postinfection with *P. berghei*. After adherence and fixation, hemocytes were stained with a PPO6 antibody (A). PPO6⁺ phagocytes (green) that have phagocytosed red fluorescent beads were compared between LP and CLD treatments (A), as well as the proportion of nonphagocytic PPO6⁺ cells (B). Closer examination of PPO6⁺ phagocytic cells revealed distinct populations of immune cells distinguished by PPO6 signal intensity (high or low) and morphological features (elongated/spread, small rounded) (C). Two independent experiments of immunofluorescent assays were performed. Data were analyzed by Mann-Whitney test using GraphPad Prism 6.0. Median is indicated by the horizontal red line (A). Bars represent mean \pm SEM (B and C). Asterisks denote significance (** $P < 0.01$, **** $P < 0.0001$). (Scale bar: 10 μ m).

blood feeding (12, 16), although the mechanisms for this increased phagocytic activity remain unknown.

Infection experiments following phagocyte depletion demonstrate the integral role of phagocytic immune cells in the mosquito immune response to bacterial and parasitic pathogens. With phagocytosis serving as the primary mechanism to remove invading pathogens, it is not surprising that mosquito survival is significantly reduced upon bacterial challenge after clodronate treatment, yet it provides an additional functional validation of the ability to deplete phagocytic immune cells in the mosquito host. Similar results were described in *Drosophila* lines devoid of phagocytic plasmatocytes (51, 52), demonstrating the conserved and vital roles of phagocytes on invertebrate survival.

These phagocyte depletion experiments have also enabled the ability to discern the specific contributions of phagocytic immune cell subtypes to malaria parasite infection. Previous work implicating mosquito hemocytes and hemocyte-derived components have been limited to reverse genetic approaches evaluating the influence of candidate gene function (14, 16, 19, 20, 23, 35) or overloading the phagocytic capacity of cells to evaluate their cellular function (22, 35). Through our experiments using CLDs, we now provide definitive evidence that phagocytic immune cells in mosquito mediate multimodal immune responses that target the ookinete and oocyst stages of malaria parasite development.

Immune recognition and lysis of invading ookinetes occurs at the interphase of the basal lamina where malaria parasite first become exposed to components of the mosquito hemolymph (25, 55). There mosquito complement recognition directs ookinete killing responses that require TEP1 function (36–38). Following phagocyte depletion, early oocyst numbers are significantly increased, suggesting that clodronate treatment increases the survival of invading ookinetes. Circulating levels of TEP1 were not altered in mosquito hemolymph following CLD treatment, yet TEP1 binding to invading ookinetes was significantly impaired. This is in agreement with recent studies (35) arguing that hemocyte-derived

microvesicles (HdMVs) are critical mediators of TEP1 binding to invading ookinetes. These studies suggest that phagocytic immune cells produce the HdMVs required for ookinete lysis.

In addition, these studies also provide information regarding the mechanisms that define oocyst survival (23–25, 39). Previous results have implicated mosquito hemocytes (23, 24), yet the application of CLDs provides direct evidence of phagocytes in mediating these oocyst killing responses. The identification of multiple PPOs that contribute to oocyst survival provide insight into the mechanisms of late-phase immunity. Gene-silencing experiments demonstrate the ability to individually target PPO genes to evaluate their contributions to malaria parasite survival. From these experiments, we identify three *PPO* genes, *PPO2*, *PPO3*, and *PPO9*, that limit the survival of *Plasmodium* oocysts. Commonly associated with melanization, the role of PPOs in oocyst killing has not been fully elucidated, but the lack of melanized oocysts in our experiments suggest a different mechanism of action. In addition to the production of melanin, PPOs have been implicated in coagulation and wound healing responses that contribute to the elimination of bacterial, viral, and parasitic pathogens (56–60). As a result, we believe that these killing responses are likely mediated by cytotoxic intermediates produced by the activation of the PO cascade (61). This includes reactive oxygen or nitrogen intermediates that may be permeable to the midgut basal lamina that otherwise protects maturing oocysts from components of the mosquito hemolymph. The exact mechanisms by which a subset of PPOs promote parasite killing have yet to be identified and are the focus of future work.

While the role of PPOs in innate immunity has been well studied in other insects (56, 62), our current understanding of PPOs in mosquitoes has been limited and further complicated by their recent gene expansion in mosquito species. *An. gambiae* has 9 annotated PPO genes, compared with only 3 identified in *Drosophila*. Based primarily on evidence from other insect systems, mosquito oenocytoid populations have predominantly

been implicated in the expression of mosquito PPOs. However, recent studies have begun to illustrate that phagocytic cell populations are also important components of mosquito PPO production (16, 45), in agreement with our results following phagocyte depletion. This is further supported by additional studies examining PPO6 transgene expression in *An. gambiae* (44, 45), and PPO staining in granulocytes of mosquitoes, moths, and houseflies (5, 11, 12, 63, 64) that together argue that phagocytic cell populations have integral roles in PPO expression and PO activity. Moreover, we believe that these differences in PPO expression highlight the need to revisit the traditional morphological classifications of mosquito hemocyte populations. Recent data by Severo et al. (45) as well as our own work, suggest that multiple phagocytic cell populations can be defined by PPO6 expression and morphological characteristics. Therefore, these insights extend well beyond the “granulocyte” classification that have previously denoted mosquito phagocytic cell populations and provide details into the complexity of these distinct cell populations.

In addition, the temporal aspects of our work examine the contributions to mosquito cellular immunity to malaria parasite killing. While clodronate treatment and subsequent phagocyte depletion before infection lead to significant increases in ookinete and oocyst survival, treatment after an established infection had no effect on malaria parasite numbers. This suggests that phagocytic immune cells are able to initiate both “early-phase” and “late-phase” immune signaling responses targeting *Plasmodium* ookinetes and oocyst numbers (Fig. 7). However, when phagocytes are depleted after ookinete invasion, the immune signals that contribute to these immune killing responses have already been set in motion, thus limiting the effects of phagocyte depletion. This is in agreement with previous models that suggest that these immune signals are initiated in response to midgut epithelial damage (23, 25), where parasites are likely killed through nonspecific to cellular damage and wound healing.

In summary, our findings are a definitive characterization of mosquito phagocytes in anti-*Plasmodium* immunity. Taking advantage of existing tools from vertebrate systems, we demonstrate that CLDs are an effective method to deplete phagocytic immune cells in *An. gambiae*, thus enabling methodologies to better understand the contributions of phagocytic immune cells to mosquito immunity. From these data, we corroborate recent studies arguing for the role of cellular immunity in directing the recognition and killing of *Plasmodium* ookinetes, as well as provide insights into the mechanisms that influence oocyst survival. This work also sheds important information into the complexity of mosquito phagocyte populations, identifying at least 3 phagocytic cell types. Together, we believe this study represents a significant advancement in our understanding of mosquito immune cells and the mechanisms by which they contribute to malaria parasite killing. Moreover, these experiments demonstrate the utility of CLDs to study immune cell populations in invertebrate systems where genetic tools are limited.

Materials and Methods

Mosquito Rearing. *An. gambiae* Keele strain mosquitoes (65, 66) were reared at 27 °C and 80% relative humidity, with a 14/10-h day/night cycle. Larvae were fed on fish flakes (Tetramin; Tetra), while adult mosquitoes were maintained on 10% sucrose solution.

Plasmodium Infection. Female Swiss Webster mice were infected with *P. berghei*-mCherry strain as described previously (23, 24). Infected mosquitoes were maintained at 19 °C until individual mosquito midguts were dissected to count oocyst numbers by fluorescence microscopy (Nikon Eclipse 50i; Nikon).

Phagocyte Depletion Using Clodronate Liposomes. Naive female mosquitoes (4- to 6-d old) were injected intrathoracically with either 69 nL of control liposomes (LPs) or CLDs (standard macrophage depletion kit; Encapsula NanoSciences) using a Nanoject II injector (Drummond Scientific). Initial experiments were performed using different dilutions of the stock concentrations using LPs and CLDs in 1× PBS (1, 1:2, 1:5, and PBS only) to determine

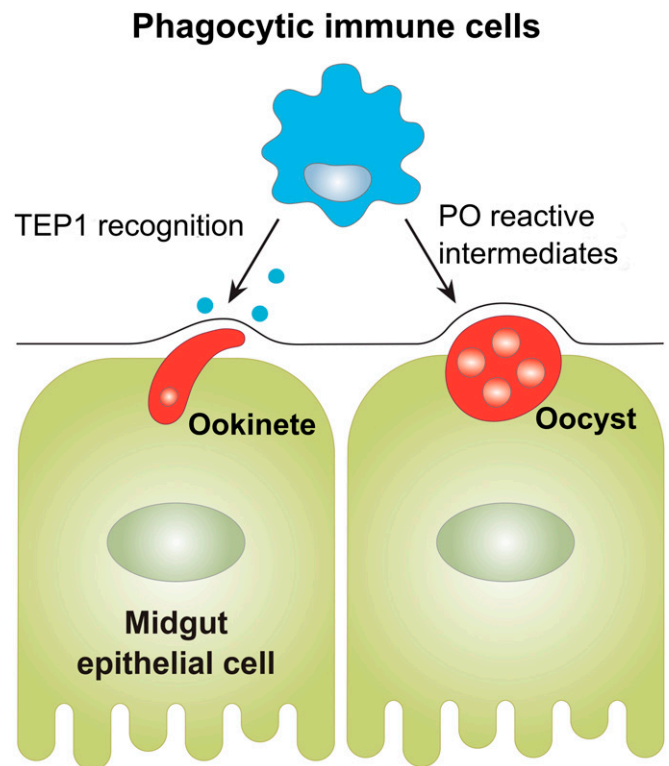


Fig. 7. Multimodal contributions of phagocytes on anti-*Plasmodium* immunity. Experiments with CLDs establish integral roles of phagocytic immune cells in malaria parasite killing, which include the role of phagocytes in the recognition of invading ookinetes and the production of PPOs that limit oocyst survival.

CLD efficacy on phagocyte depletion and its effects on mosquito survival. All subsequent experiments were performed using a 1:5 dilution of control or CLDs in 1× PBS. Liposome injections were performed either on naive mosquitoes 1 d before blood feeding or *P. berghei* challenge (pretreatment), or on mosquitoes 24 h after *P. berghei* infection (posttreatment).

Hemolymph Perfusion and Hemocyte Counting. Hemolymph perfusion and hemocyte counting were performed as previously described (23, 24). Hemolymph was collected from pretreated mosquitoes at 24 h (24-h naive), 48-h naive, 24-h blood-fed (24-h BF), 24-h *P. berghei* infection (24-h *P.b*) and post-treated mosquitoes at 48-h *P. berghei* infection (48-h *P.b*) using anticoagulant solution (60% [vol/vol] Schneider's insect medium, 10% FBS, and 30% citrate buffer; 98 mM NaOH, 186 mM NaCl, 1.7 mM EDTA, and 41 mM citric acid, pH 4.5) as described previously (23, 24). Hemolymph (10 μ L) from an individual mosquito was perfused through an incision made in the lateral abdomen. Hemocytes were quantified counting ~200 cells per individual mosquito, and the hemocyte subtypes were evaluated by morphological differences using a disposable Neubauer hemocytometer slide (C-Chip DHC-N01; INCYTO).

In Vivo Hemocyte Staining Using CM-Dil To visualize the depletion of phagocytes following CLD treatment, hemocytes were stained as previously using CM-Dil (Vybrant CM-Dil; Life Technologies) and FITC-conjugated WGA (Sigma) (5, 9, 13, 22, 23, 35). Both CM-Dil and WGA have been previously used as “universal” stains to label mosquito hemocyte populations (5, 9, 13, 22, 23, 35). CM-Dil is a lipophilic dye that specifically labels mosquito hemocytes (9, 13), while WGA is a lectin that recognizes *N*-acetylglucosamine modifications common to many membrane-bound glycoproteins commonly found on mosquito hemocytes (5). Briefly, mosquitoes pretreated with either control liposomes or CLDs were challenged with *P. berghei*, then ~24 h postinfection were injected with 138 nL of 100 μ M CM-Dil and incubated for 20 min at 19 °C. Perfused hemolymph (~10 μ L) was collected onto a multitest glass slide (MP Biomedicals), and hemocytes were allowed to adhere to the slide for 30 min. Without washing, 4% paraformaldehyde was added to each well for fixation. After incubating at room temperature (RT) for 30 min, cells were washed three times in 1× PBS for 5 min, and then blocked with 1% BSA in 1× PBS for 30 min before incubating with WGA (1:500) overnight at 4 °C. Before visualization,

slides were washed 3 times in 1× PBS for 5 min, and then mounted with ProLongDiamond Antifade mountant with DAPI (Life Technologies).

Flow Cytometry. Flow cytometry analyses was performed to confirm phagocyte depletion following CLD treatment. Mosquitoes pretreated with CLD under naive, 24-h blood-fed, or 24-h *P. berghei*-infected conditions were injected with red fluorescent FluoSpheres (1 μm; Molecular Probes) at a final concentration of 2% (vol/vol) and allowed to recover for 2 h at 19 °C before perfusion. Hemolymph was collected from ~60 individual mosquitoes for each experimental treatment as described above using anticoagulant solution as previously described (23, 24). Perfused cell samples were fixed in 4% paraformaldehyde for 1 h at 4 °C, and then centrifuged for 5 min at 2,000 × g to pellet cells, while discarding the supernatant. Cells were washed two times in 1× PBS with an additional centrifugation step of 5 min at 2,000 × g between washing steps. Samples were incubated with WGA (1:5,000) and DRAQ5 (1:1,000; Thermo Fisher Scientific) overnight at 4 °C. Following incubation, cells were washed two times in 1× PBS to remove excess stain, and then run on a BD FACSCanto cytometer (BD Biosciences). Data were analyzed with FlowJo software (FlowJo) using strict threshold values for gating as determined by a fluorescent bead-only sample to exclude events by size (FSC) and the use of unstained cells to determine cutoffs for positive WGA and DRAQ5 signals to remove any autofluorescence background. To measure the effects of CLD depletion, the percentage of phagocytic cells in LP and CLD samples were used for comparison. Flow cytometry experiments were performed 3 or more times from independent biological experiments for naive, blood-fed, and *P. berghei*-infected conditions.

RNA Isolation and Gene Expression Analyses. Total RNA was isolated from dissected mosquito tissues or from whole mosquito samples to examine gene expression using TRIzol (Thermo Fisher Scientific). Two micrograms of total RNA were used as a template for cDNA synthesis using the RevertAid First Strand cDNA Synthesis kit (Thermo Fisher Scientific). qRT-PCR was performed using PowerUpSYBRGreen Master Mix (Thermo Fisher Scientific) with the ribosomal S7 protein transcript serving as an internal reference as previously (24). cDNA (1:5 dilution) amplification was performed with 250 nM of each specific primer pair using the following cycling conditions: 95 °C for 10 min, 40 cycles with 95 °C for 15 s and 65 °C for 60 s. A comparative C_T ($2^{-\Delta\Delta C_T}$) method was employed to evaluate relative transcript abundance for each transcript (67). A list of primers used for gene expression analyses are listed in *SI Appendix, Table S2*.

Phagocytosis Assays. Phagocytosis assays were performed by injecting 69 nL of red fluorescent FluoSpheres at final concentration of 2% (vol/vol) into naive, 24-h blood-fed, or 24-h *P. berghei*-infected mosquitoes as previously (23). Following injection, mosquitoes were kept at 19 °C for 2 h before hemolymph was perfused onto a multitest glass slide. Hemocytes were allowed to attach the slide for 30 min at RT and were then fixed with 4% paraformaldehyde for 30 min. Slides were washed 3 times in 1× PBS for 5 min each wash, and then blocked in 1% of BSA for 30 min. To visualize cells, samples were incubated with 1:500 WGA overnight at 4 °C. Hemocytes were washed 3 times in 1× PBS, and then mounted with ProLongDiamond Antifade mountant with DAPI. Hemocytes labeled with WGA and harboring red fluorescent beads were considered as phagocytes. Phagocytic activity was evaluated as the number of immune cells engulfing 1 or more fluorescent beads divided by total immune cell population ($n = 50/\text{mosquito}$) counted from random chosen fields under a fluorescent microscope. The average number of fluorescent beads per phagocyte was also determined and is referred to as the phagocytic index.

Bacterial Challenge Experiments. Bacteria were grown in LB media overnight at 37 °C with 210 rpm. Bacterial cultures were centrifuged at 8,000 rpm for 5 min, washed twice with 1× PBS, and resuspended in 1× PBS. Approximately 24 h after pretreatment with control or CLDs, mosquitoes ($n = 30$) were injected with 69 nL of bacterial suspensions (100× dilution of the $OD_{600} = 0.4$ suspension; *Serratia marcescens* [$2.2 \times 10^8/\text{mL}$] or *Staphylococcus aureus* [$6.3 \times 10^8/\text{mL}$]) using a nanoinjector. Mosquitoes pretreated with control and CLDs were also injected with 69 nL of 1× PBS to serve as an additional control to measure the effects of injury on mortality. Following challenge, mosquitoes were maintained at 27 °C and 80% relative humidity with mosquito survival monitored every 24 h for 10 d.

TEP1 Immunofluorescence Assays. Analysis of TEP1 binding to invading ookinetes was performed by immunofluorescence similar to previous experiments (35, 38, 68, 69). Mosquitoes pretreated with liposomes and infected with *P. berghei* were dissected at ~22–24 h postinfection. Midguts were dissected and briefly fixed in 4% paraformaldehyde for 40 s, and then the blood bolus was removed and the midguts briefly washed in 1× PBS

before fixation in 4% PFA for 1 h at RT. Following washing 3 times in 1× PBS, midguts were blocked in blocking buffer (1% BSA and 0.1% Triton X-100 in 1× PBS) overnight at 4 °C. Midgut sheets were incubated with mouse α -Pbs21 (1:500) and rabbit-TEP1 (1:500) primary antibodies in blocking buffer overnight at 4 °C. After washing in 1× PBS, midguts were incubated with Alexa Fluor 568 goat anti-mouse IgG (1:500; Thermo Fisher Scientific) and Alexa Fluor 488 goat anti-rabbit IgG (1:500; Thermo Fisher Scientific) secondary antibodies in blocking buffer for 2 h at RT. Midguts were washed 3 times in 1× PBS, and then mounted with ProLongDiamond Antifade mountant with DAPI.

RNA-Seq and Differential Gene Expression Analysis. Adult female mosquitoes were pretreated with either control or CLDs as described above, and then challenged with *P. berghei*. Approximately 24 h postinfection, mosquitoes were dissected in 1× PBS to dissociate the gut and reproductive organs from the abdominal wall. Total RNA was extracted from dissected abdomen ($n = 15$) tissues using TRIzol (Thermo Fisher Scientific) for each treatment. The isolated RNA was further purified with the RNA Clean & Concentrator-5 kit (Zymo Research) and quantified using a Nanodrop spectrophotometer (Thermo Fisher Scientific). RNA quality and integrity were measured using an Agilent 2100 Bioanalyzer Nano Chip (Agilent Technologies), and 200 ng of total RNA from 4 independent biological replicates was used to perform RNA-seq analysis. Additional experimental details are described in *SI Appendix*.

Gene Silencing by dsRNA. RNAi experiments were performed as previously described (23, 24, 70). Additional experimental details are described in *SI Appendix*.

PO Assay. PO activity was measured in pools of perfused hemolymph from pretreated mosquitoes ($n = 15$; 10 μL per mosquito) under naive conditions, 24 h postblood feeding, and 24 h post-*P. berghei* infection. Following perfusion, 10 μL of the total perfused hemolymph was mixed with 90 μL of 3,4-dihydroxy-L-phenylalanine (L-DOPA) (4 mg/mL) dissolved in nuclease-free water as previously described (71). PO activity was measured at 490 nm every 5 min for 30 min, and then the final activity was measured at 60 min using a microplate reader.

Western Blot Analysis. Experimental details are described in the *SI Appendix*.

Hemocyte Immunofluorescence Assays. Hemocyte immunofluorescence assays were performed using a PPO6 antibody as previously described (11, 12). Mosquitoes pretreated with either control liposomes or CLDs were injected with red fluorescent FluoSpheres at a final concentration of 2% (vol/vol) ~24 h after *P. berghei* infection. Following incubation for 2 h at 19 °C, hemocytes were perfused on a multiwell glass slide and allowed to adhere at RT for 30 min. Cells were fixed with 4% paraformaldehyde for 30 min, and then washed 3 times in 1× PBS. Samples were incubated with blocking buffer (0.1% Triton X-100, 1% BSA in PBS) for 1 h at RT and incubated with rabbit-anti PPO6 (1:500) in blocking buffer overnight at 4 °C. After washing 3 times in 1× PBS, an Alexa Fluor 488 goat anti-rabbit IgG (1:500) secondary antibody was added in blocking buffer for 2 h at RT. Slides were rinsed 3 times in 1× PBS and mounted with ProLongDiamond Antifade mountant with DAPI. Hemocytes were screened for the presence of PPO6 signal and phagocytic activity. The percentage of PPO6⁺ cells displaying phagocytic ability were counted as a proportion of the total cell population. Approximately 200 randomly selected hemocytes were evaluated in liposome controls, while the entire cell population was counted in CLD-treated samples with less than 200 cells. Discernable differences in phagocyte populations between control and CLD-treated samples were determined based on morphology. The intensity of PPO6 fluorescence was determined by measuring the integrated pixel density from individual images using ImageJ software (<https://imagej.nih.gov/ij/>).

ACKNOWLEDGMENTS. We thank Andrea Radtke for the initial discussions that led this project. This work would not have been possible without the generosity of Kristin Michel for sharing the SRPN3 antibody, to Michael Povelones for providing the TEP1 antibody, and to George Christophides for offering the PPO6 antibody used in these studies. We thank Linda Zeller for providing the *S. marcescens* and *S. aureus* bacterial cultures, and offer a special thanks to Shaun Rigby of the Iowa State Flow Cytometry Facility for his instrumental help in performing flow cytometry experiments. We also thank Arun Somwarpet-Seetharam and Andrew Severin of the Iowa State Genome Informatics Facility for assistance with the gene expression data; Mike Baker of the Iowa State DNA Core Facility for assistance with the RNA-seq project; and Hee Jung Oh for assistance in scientific illustrations. This research was supported in part by the Agricultural Experiment Station at Iowa State University.

1. M. Salzet, Vertebrate innate immunity resembles a mosaic of invertebrate immune responses. *Trends Immunol.* **22**, 285–288 (2001).
2. K. S. Gold, K. Brückner, Macrophages and cellular immunity in *Drosophila melanogaster*. *Semin. Immunol.* **27**, 357–368 (2015).
3. M. J. Williams, *Drosophila* hemopoiesis and cellular immunity. *J. Immunol.* **178**, 4711–4716 (2007).
4. V. Honti, G. Csordás, É. Kurucz, R. Márkus, I. Andó, The cell-mediated immunity of *Drosophila melanogaster*: Hemocyte lineages, immune compartments, microanatomy and regulation. *Dev. Comp. Immunol.* **42**, 47–56 (2014).
5. J. C. Castillo, A. E. Robertson, M. R. Strand, Characterization of hemocytes from the mosquitoes *Anopheles gambiae* and *Aedes aegypti*. *Insect Biochem. Mol. Biol.* **36**, 891–903 (2006).
6. J. F. Hillyer, M. R. Strand, Mosquito hemocyte-mediated immune responses. *Curr. Opin. Insect Sci.* **3**, 14–21 (2014).
7. M. D. Lavine, M. R. Strand, Insect hemocytes and their role in immunity. *Insect Biochem. Mol. Biol.* **32**, 1295–1309 (2002).
8. J. F. Hillyer, S. L. Schmidt, B. M. Christensen, Hemocyte-mediated phagocytosis and melanization in the mosquito *Armigeres subalbatus* following immune challenge by bacteria. *Cell Tissue Res.* **313**, 117–127 (2003).
9. J. G. King, J. F. Hillyer, Spatial and temporal in vivo analysis of circulating and sessile immune cells in mosquitoes: Hemocyte mitosis following infection. *BMC Biol.* **11**, 55 (2013).
10. J. Castillo, M. R. Brown, M. R. Strand, Blood feeding and insulin-like peptide 3 stimulate proliferation of hemocytes in the mosquito *Aedes aegypti*. *PLoS Pathog.* **7**, e1002274 (2011).
11. W. B. Bryant, K. Michel, Blood feeding induces hemocyte proliferation and activation in the African malaria mosquito, *Anopheles gambiae* Giles. *J. Exp. Biol.* **217**, 1238–1245 (2014).
12. W. B. Bryant, K. Michel, *Anopheles gambiae* hemocytes exhibit transient states of activation. *Dev. Comp. Immunol.* **55**, 119–129 (2016).
13. J. G. King, J. F. Hillyer, Infection-induced interaction between the mosquito circulatory and immune systems. *PLoS Pathog.* **8**, e1003058 (2012).
14. S. B. Pinto et al., Discovery of *Plasmodium* modulators by genome-wide analysis of circulating hemocytes in *Anopheles gambiae*. *Proc. Natl. Acad. Sci. U.S.A.* **106**, 21270–21275 (2009).
15. L. A. Baton, A. Robertson, E. Warr, M. R. Strand, G. Dimopoulos, Genome-wide transcriptomic profiling of *Anopheles gambiae* hemocytes reveals pathogen-specific signatures upon bacterial challenge and *Plasmodium berghei* infection. *BMC Genomics* **10**, 257 (2009).
16. R. C. Smith et al., Molecular profiling of phagocytic immune cells in *Anopheles gambiae* reveals integral roles for hemocytes in mosquito innate immunity. *Mol. Cell. Proteomics* **15**, 3373–3387 (2016).
17. L. F. Moita et al., In vivo identification of novel regulators and conserved pathways of phagocytosis in *A. gambiae*. *Immunity* **23**, 65–73 (2005).
18. F. Lombardo, Y. Ghani, F. C. Kafatos, G. K. Christophides, Comprehensive genetic dissection of the hemocyte immune response in the malaria mosquito *Anopheles gambiae*. *PLoS Pathog.* **9**, e1003145 (2013).
19. F. Lombardo, G. K. Christophides, Novel factors of *Anopheles gambiae* haemocyte immune response to *Plasmodium berghei* infection. *Parasit. Vectors* **9**, 78 (2016).
20. J. L. Ramirez et al., The role of hemocytes in *Anopheles gambiae* antiplasmodial immunity. *J. Innate Immun.* **6**, 119–128 (2014).
21. J. L. Ramirez et al., A mosquito lipoxin/lipocalin complex mediates innate immune priming in *Anopheles gambiae*. *Nat. Commun.* **6**, 7403 (2015).
22. J. Rodrigues, F. A. Brayner, L. C. Alves, R. Dixit, C. Barillas-Mury, Hemocyte differentiation mediates innate immune memory in *Anopheles gambiae* mosquitoes. *Science* **329**, 1353–1355 (2010).
23. R. C. Smith, C. Barillas-Mury, M. Jacobs-Lorena, Hemocyte differentiation mediates the mosquito late-phase immune response against *Plasmodium* in *Anopheles gambiae*. *Proc. Natl. Acad. Sci. U.S.A.* **112**, E3412–E3420 (2015).
24. H. Kwon, B. R. Arends, R. C. Smith, Late-phase immune responses limiting oocyst survival are independent of TEPI function yet display strain specific differences in *Anopheles gambiae*. *Parasit. Vectors* **10**, 369 (2017).
25. R. C. Smith, C. Barillas-Mury, *Plasmodium* oocysts: Overlooked targets of mosquito immunity. *Trends Parasitol.* **32**, 979–990 (2016).
26. P. P. Lehenkari et al., Further insight into mechanism of action of clodronate: Inhibition of mitochondrial ADP/ATP translocase by a nonhydrolyzable, adenine-containing metabolite. *Mol. Pharmacol.* **61**, 1255–1262 (2002).
27. M. B. Jordan, N. Van Rooijen, S. Izui, J. Kappler, P. Marrack, Liposomal clodronate as a novel agent for treating autoimmune hemolytic anemia in a mouse model. *Blood* **101**, 594–601 (2003).
28. N. van Rooijen, E. Hendrikx, Liposomes for specific depletion of macrophages from organs and tissues. *Methods Mol. Biol.* **605**, 189–203 (2010).
29. J. D. Oliver, J. Dusty Loy, G. Parikh, L. Bartholomay, Comparative analysis of hemocyte phagocytosis between six species of arthropods as measured by flow cytometry. *J. Invertebr. Pathol.* **108**, 126–130 (2011).
30. C. Kocks et al., Eater, a transmembrane protein mediating phagocytosis of bacterial pathogens in *Drosophila*. *Cell* **123**, 335–346 (2005).
31. E. Kurucz et al., Nimrod, a putative phagocytosis receptor with EGF repeats in *Drosophila* plasmatocytes. *Curr. Biol.* **17**, 649–654 (2007).
32. J. Midega et al., Discovery and characterization of two Nimrod superfamily members in *Anopheles gambiae*. *Pathog. Glob. Health* **107**, 463–474 (2013).
33. T. Y. Estévez-Lao, J. F. Hillyer, Involvement of the *Anopheles gambiae* Nimrod gene family in mosquito immune responses. *Insect Biochem. Mol. Biol.* **44**, 12–22 (2014).
34. Y. Hashimoto et al., Identification of lipoteichoic acid as a ligand for draper in the phagocytosis of *Staphylococcus aureus* by *Drosophila* hemocytes. *J. Immunol.* **183**, 7451–7460 (2009).
35. J. C. Castillo, A. B. B. Ferreira, N. Trisnadi, C. Barillas-Mury, Activation of mosquito complement antiplasmodial response requires cellular immunity. *Sci. Immunol.* **2**, eaal1505 (2017).
36. S. Blandin et al., Complement-like protein TEPI is a determinant of vectorial capacity in the malaria vector *Anopheles gambiae*. *Cell* **116**, 661–670 (2004).
37. M. Fraiture et al., Two mosquito LRR proteins function as complement control factors in the TEPI-mediated killing of *Plasmodium*. *Cell Host Microbe* **5**, 273–284 (2009).
38. M. Povelones, R. M. Waterhouse, F. C. Kafatos, G. K. Christophides, Leucine-rich repeat protein complex activates mosquito complement in defense against *Plasmodium* parasites. *Science* **324**, 258–261 (2009).
39. L. Gupta et al., The STAT pathway mediates late-phase immunity against *Plasmodium* in the mosquito *Anopheles gambiae*. *Cell Host Microbe* **5**, 498–507 (2009).
40. E. Foley, P. H. O'Farrell, Nitric oxide contributes to induction of innate immune responses to gram-negative bacteria in *Drosophila*. *Genes Dev.* **17**, 115–125 (2003).
41. S. C. Wu, C. W. Liao, R. L. Pan, J. L. Juang, Infection-induced intestinal oxidative stress triggers organ-to-organ immunological communication in *Drosophila*. *Cell Host Microbe* **11**, 410–417 (2012).
42. H. Kwon, R. C. Smith, Effects of hemocyte ablation on fat body gene expression. *Gene Expression Omnibus*. <https://www.ncbi.nlm.nih.gov/geo/query/acc.cgi?acc=GSE116156>. Deposited 22, June 2018.
43. M. M. A. Whitten, C. J. Coates, Re-evaluation of insect melanogenesis research: Views from the dark side. *Pigment Cell Melanoma Res.* **30**, 386–401 (2017).
44. G. Volohonsky et al., Transgenic expression of the anti-parasitic factor TEPI in the malaria mosquito *Anopheles gambiae*. *PLoS Pathog.* **13**, e1006113 (2017).
45. M. S. Severo et al., Unbiased classification of mosquito blood cells by single-cell genomics and high-content imaging. *Proc. Natl. Acad. Sci. U.S.A.* **115**, E7568–E7577 (2018).
46. L. T. Sigle, J. F. Hillyer, Mosquito hemocytes preferentially aggregate and phagocytose pathogens in the peristrial regions of the heart that experience the most hemolymph flow. *Dev. Comp. Immunol.* **55**, 90–101 (2016).
47. K. S. Gold, K. Brückner, *Drosophila* as a model for the two myeloid blood cell systems in vertebrates. *Exp. Hematol.* **42**, 717–727 (2014).
48. A. Holz, B. Bossinger, T. Strasser, W. Janning, R. Klapper, The two origins of hemocytes in *Drosophila*. *Development* **130**, 4955–4962 (2003).
49. A. Braun, B. Lemaître, R. Lanot, D. Zachary, M. Meister, *Drosophila* immunity: Analysis of larval hemocytes by P-element-mediated enhancer trap. *Genetics* **147**, 623–634 (1997).
50. A. Braun, J. A. Hoffmann, M. Meister, Analysis of the *Drosophila* host defense in domino mutant larvae, which are devoid of hemocytes. *Proc. Natl. Acad. Sci. U.S.A.* **95**, 14337–14342 (1998).
51. A. Defaye et al., Genetic ablation of *Drosophila* phagocytes reveals their contribution to both development and resistance to bacterial infection. *J. Innate Immun.* **1**, 322–334 (2009).
52. B. Charroux, J. Royet, Elimination of plasmatocytes by targeted apoptosis reveals their role in multiple aspects of the *Drosophila* immune response. *Proc. Natl. Acad. Sci. U.S.A.* **106**, 9797–9802 (2009).
53. M. Stofanko, S. Y. Kwon, P. Badenhorst, A misexpression screen to identify regulators of *Drosophila* larval hemocyte development. *Genetics* **180**, 253–267 (2008).
54. J. F. Hillyer, S. L. Schmidt, B. M. Christensen, Rapid phagocytosis and melanization of bacteria and *Plasmodium* sporozoites by hemocytes of the mosquito *Aedes aegypti*. *J. Parasitol.* **89**, 62–69 (2003).
55. R. C. Smith, J. Vega-Rodríguez, M. Jacobs-Lorena, The *Plasmodium* bottleneck: Malaria parasite losses in the mosquito vector. *Mem. Inst. Oswaldo Cruz* **109**, 644–661 (2014).
56. O. Binggeli, C. Neyen, M. Poidevin, B. Lemaître, Prophenoloxidase activation is required for survival to microbial infections in *Drosophila*. *PLoS Pathog.* **10**, e1004067 (2014).
57. J. Rodríguez-Andrés et al., Phenoloxidase activity acts as a mosquito innate immune response against infection with Semliki Forest virus. *PLoS Pathog.* **8**, e1002977 (2012).
58. P. Zhao, Z. Lu, M. R. Strand, H. Jiang, Antiviral, anti-parasitic, and cytotoxic effects of 5,6-dihydroxyindole (DHI), a reactive compound generated by phenoloxidase during insect immune response. *Insect Biochem. Mol. Biol.* **41**, 645–652 (2011).
59. L. Cerenius, B. L. Lee, K. Söderhäll, The proPO-system: Pros and cons for its role in invertebrate immunity. *Trends Immunol.* **29**, 263–271 (2008).
60. Z. Zou et al., Mosquito RUNX4 in the immune regulation of PPO gene expression and its effect on avian malaria parasite infection. *Proc. Natl. Acad. Sci. U.S.A.* **105**, 18454–18459 (2008).
61. A. J. Nappi, B. M. Christensen, Melanogenesis and associated cytotoxic reactions: Applications to insect innate immunity. *Insect Biochem. Mol. Biol.* **35**, 443–459 (2005).
62. J. P. Dudzic, S. Kondo, R. Ueda, C. M. Bergman, B. Lemaître, *Drosophila* innate immunity: Regional and functional specialization of prophenoloxidases. *BMC Biol.* **13**, 81 (2015).
63. Z. Wang et al., A systematic study on hemocyte identification and plasma prophenoloxidase from *Culex pipiens quinquefasciatus* at different developmental stages. *Exp. Parasitol.* **127**, 135–141 (2011).
64. E. Ling, X. Q. Yu, Prophenoloxidase binds to the surface of hemocytes and is involved in hemocyte melanization in *Manduca sexta*. *Insect Biochem. Mol. Biol.* **35**, 1356–1366 (2005).
65. H. Hurd, P. J. Taylor, D. Adams, A. Underhill, P. Eggleston, Evaluating the costs of mosquito resistance to malaria parasites. *Evolution* **59**, 2560–2572 (2005).
66. L. C. Ranford-Cartwright et al., Characterisation of species and diversity of *Anopheles gambiae* Keele colony. *PLoS One* **11**, e0168999 (2016).
67. K. J. Livak, T. D. Schmittgen, Analysis of relative gene expression data using real-time quantitative PCR and the 2(-Delta Delta C(T)) method. *Methods* **25**, 402–408 (2001).
68. Gde. A. Oliveira, J. Lieberman, C. Barillas-Mury, Epithelial nitration by a peroxidase/NOX5 system mediates mosquito antiplasmodial immunity. *Science* **335**, 856–859 (2012).
69. M. Povelones et al., The CLIP-domain serine protease homolog SPCLIP1 regulates complement recruitment to microbial surfaces in the malaria mosquito *Anopheles gambiae*. *PLoS Pathog.* **9**, e1003623 (2013).
70. R. C. Smith, A. G. Eappen, A. J. Radtke, M. Jacobs-Lorena, Regulation of anti-*Plasmodium* immunity by a LITAF-like transcription factor in the malaria vector *Anopheles gambiae*. *PLoS Pathog.* **8**, e1002965 (2012).
71. G. P. League, T. Y. Estévez-Lao, Y. Yan, V. A. García-Lopez, J. F. Hillyer, *Anopheles gambiae* larvae mount stronger immune responses against bacterial infection than adults: Evidence of adaptive decoupling in mosquitoes. *Parasit. Vectors* **10**, 367 (2017).